

Preclinical Studies of Pegylated- and Non-Pegylated Liposomal Forms of Doxorubicin as Radiosensitizer on Orthotopic High-Grade Glioma Xenografts

P. Chastagner · H. Sudour · J. Mriouah · M. Barberi-Heyob · V. Bernier-Chastagner · S. Pinel

Received: 19 February 2014 / Accepted: 2 July 2014 / Published online: 22 July 2014
© Springer Science+Business Media New York 2014

ABSTRACT

Purpose Free doxorubicin (DXR) is not currently used to treat brain tumors because (i) the blood–brain barrier limits the drug deposition into the brain (ii) lethal toxic effects occur when combined with radiation therapy. Since encapsulation of DXR within liposomal carriers could overcome these drawbacks, the present study aimed at evaluating the radiosensitizing properties of non-pegylated (NPL-DXR) and pegylated (PL-DXR) liposomal doxorubicin on orthotopic high-grade glioma xenografts (U87).

Methods DXR accumulation in brain tissues was assessed by a high-performance liquid chromatography method and antitumor efficacy was evaluated by mice survival determination.

Results We showed that encapsulation of DXR ensured a preferential deposition of DXR in tumoral tissue in comparison with normal brain tissue: the best AUC tumor tissue/AUC normal tissue *ratio* depended greatly on the schedule. Overall, thanks to the optimization of the delivery schedule, we demonstrated a radiosensitizing effect for both liposomal DXR without toxicity of this combination on the U87 human malignant glioma orthotopic xenografts.

Conclusion This study shows that the use of nanocarriers, allowing targeting of intracerebral tumor, renders relevant the combination of anthracyclin with radiation therapy to treat brain tumors, opening a new field of therapeutic applications. However, our results point out that, for each new delivery system, the administration schedules need to be rigorously optimized.

KEY WORDS brain distribution · high-grade glioma · liposomal doxorubicin · radiosensitization · radiotherapy

ABBREVIATIONS

AUC	Area under the curve
BBB	Blood–brain barrier
BTB	Blood–tumor barrier
CNS	Central nervous system
DXR	Doxorubicin
MTD	maximal tolerated dose
NPL-DXR	Non-pegylated liposomal doxorubicin
NT	Non-tumor brain hemisphere
PL-DXR	Pegylated liposomal doxorubicin
RT	Radiotherapy
TT	Tumor brain hemisphere

INTRODUCTION

Current standard treatment of patients harboring malignant gliomas consists of surgical removal of the tumor, followed by concomitant chemotherapy and radiotherapy (RT). Glioblastoma patients with the most favorable combination of prognostic factors receiving combined radiochemotherapy have a median overall survival of 8.3–16.6 months [1]. In these malignancies, the main challenge concerns the eradication of

P. Chastagner · J. Mriouah · M. Barberi-Heyob · S. Pinel
Université de Lorraine, CRAN UMR 7039 Campus Sciences BP70239
Vandoeuvre-les-Nancy 54500, France

P. Chastagner · J. Mriouah · M. Barberi-Heyob · S. Pinel
CNRS, CRAN, UMR 7039 Campus Sciences BP70239
Vandoeuvre-les-Nancy 54500, France

P. Chastagner · H. Sudour
CHRU Nancy, Hôpital d'Enfants-Service d'Oncologie et Hématologie
Pédiatriques Vandoeuvre-les-Nancy 54500, France

V. Bernier-Chastagner
Département de Radiothérapie, Institut de Cancérologie de Lorraine
Avenue de Bourgogne Vandoeuvre-les-Nancy 54500, France

S. Pinel (✉)
Faculté de Médecine, CRAN, UMR 7039 UL - CNRS 9 avenue de la
Forêt de Haye 54500 Vandoeuvre-les-Nancy, France
e-mail: sophie.pinel@univ-lorraine.fr

the infiltrative glioma cells that persist after the subtotal surgical resection. Chemotherapy has not consistently demonstrated favorable results with response rates regularly less than 20%. Poor penetration of most anticancer drugs across the blood–brain barrier (BBB) into the central nervous system (CNS), impairing the destruction of residual microscopic tumor cells, is one of the major reasons why improvement of survival is limited. Moreover, the blood-tumor barrier (BTB), more permeable than the BBB, still limits the amount of potent agents that can be delivered to the tumor: the selective permeability of BTB blocks many antitumor drugs which are unable to reach therapeutic level in tumor tissue [2].

Doxorubicin is one of the most effective agent *in vitro* [3, 4] and *in vivo* studies have demonstrated that DXR, when delivered locally, was an effective therapeutic agent against experimental intracranial gliomas [5]. However, because of very poor penetration across the BBB and BTB, systemic delivery of DXR has not been used for treatment of brain tumor patients, whereas a phase I clinical trial evaluating intralesional administration of doxorubicin in recurrent malignant gliomas confirmed the efficacy of anthracyclin to treat brain tumor [6].

To overcome the high toxicity and increase the penetration of doxorubicin, investigators have developed liposomal encapsulated forms. These liposomal encapsulations using pegylated forms (PL-DXR) have been shown to significantly improve the penetration of doxorubicin across the BTB in animal tumor models compared with free doxorubicin [7, 8]. Clinical trials evaluating intravenous administration of PL-DXR for patients with recurrent high-grade glioblastoma demonstrated a potential application in the treatment of glioblastomas [9, 10]. Liposomal DXR has also been demonstrated to enhance the therapeutic effect of RT in several animal tumor models [11–13] but our previous results in high-grade glioma were somewhat contradictory, likely due to the lack of treatment optimization [14]. To evaluate the radiosensitizing properties of liposomal forms of DXR, we performed a study comparing for the first time the biodistribution and efficiency of NPL-DXR and PL-DXR on orthotopic high-grade glioma xenografts. However, because NPL-DXR and PL-DXR have very different pharmacokinetics and toxicity profiles in humans, we designed a study to assess their radiosensitizing efficiency when used at the maximum tolerated dose.

MATERIALS AND METHODS

Anticancer Drugs

In the present study, NPL-DXR and PL-DXR were Myocet® (Cephalon) and Caelyx® (Schering Plough), respectively. Myocet® and Caelyx® are both commercialized liposomal

forms of doxorubicin usually delivered in clinical practice. Intravenous route was used to deliver these drugs.

Animals and Tumors

Pathogen-free, 5–7 week-old female athymic NMRI-nu (*nu/nu*) mice were purchased from Janvier Laboratories (Le-Genest-St-Isle, France). Research adhered to the “Principles of Laboratory Animal Care” (NIH publication #85-23, revised in 1985). Animals were housed in solid-bottomed plastic cages (6 mice per cage) with free access to tap water and food *ad libitum*. All experiments were performed in accordance with animal care guidelines (Directive 2010/63/EU) and carried out by competent and authorized persons (personal authorization number 54–89 issued by the Department of Veterinary Services) in a registered establishment (establishment number C-54-547-03 issued by the Department of Veterinary Services). All surgical and MRI procedures were carried out under general anesthesia obtained by intraperitoneal (i.p.) injection of xylazine (8 mg/kg) and ketamine (90 mg/kg). Tumor xenografts were obtained as described earlier [15]. The U87 model (HTB-14, American Type Culture Collection, USA) was maintained *in vivo* by sequential passages of tumor fragments in nude mice.

Grafts

For the experiments, source tumors were excised, cleaned from necrotic tissue, cut into small fragments and subcutaneously or intracranially implanted into each experimental mouse. For intracranial graft, a craniotomy flap was made and raised, after opening the mouse’s skull skin. A 1-mm³ graft was then slid under the meninges and into the brain cortex in its temporo-occipital area. MRI imaging were conducted on a Bruker Biospec Avance 24/40NMR spectro-imager (Bruker Biospin, Ettlingen, Germany) at 2.35 T using a T1-weighted spin–echo sequence and gadolinium contrast enhancement, as previously described [14].

Determination of Equitoxic Doses of NPL-DXR and PL-DXR

To define the equitoxic dose of NPL-DXR and PL-DXR, we investigated first the maximal tolerated dose (MTD) for each drug using escalating doses.

The MTD refers to the highest dose that induced neither toxic death during the 40 days after treatment onset, nor weight loss more than 10% of initial body weight. This threshold on weight loss was chosen because in our experience, a more severe weight loss was life-threatening and could compromise the radiosensitization study.

We designed two treatment schedules (Fig. 1): the first schedule consisted in 2 injections/week \times 2 weeks, and the second one in 3 injections/week \times 2 weeks. The first dose level

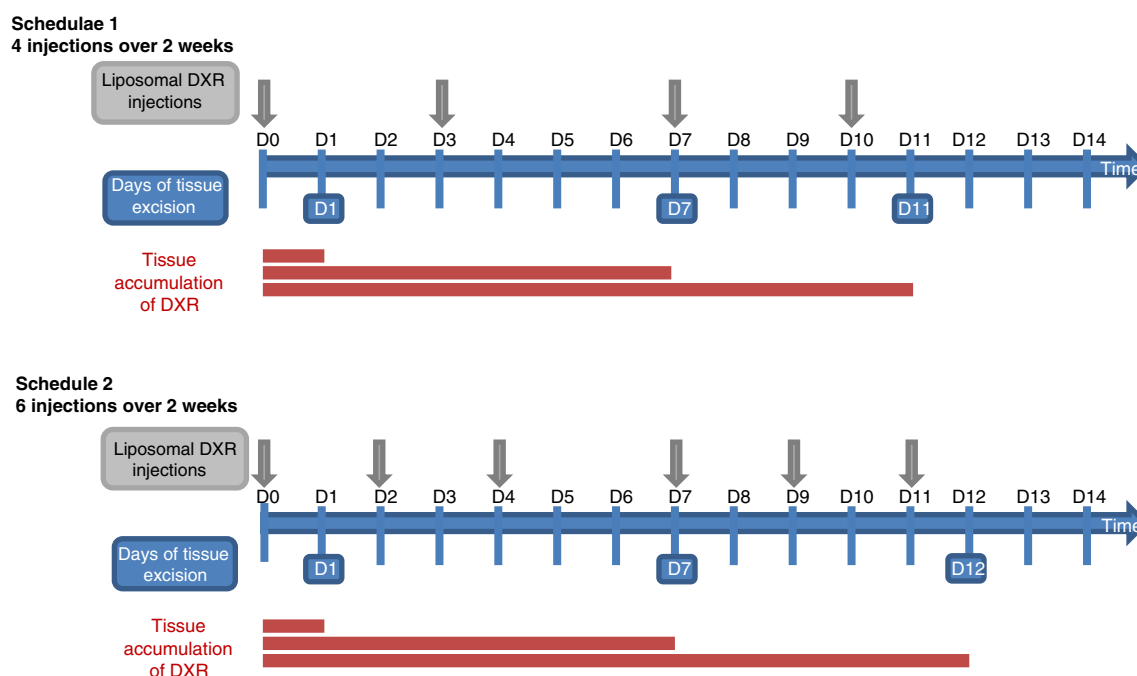


Fig. 1 Experimental protocols for NPL-DXR and PL-DXR brain distribution and radiosensitizing efficacy. When presence of tumor was observed on MRI examination, mice were randomly assigned into therapeutic groups and treatments started, corresponding to the day (D0). In distribution study, NPL-DXR and PL-DXR were delivered at equitoxic doses (total doses of 24 and 15 mg/kg, respectively), according to 2 schedules (4 injections or 6 injections over 2 weeks). To compare DXR accumulation in brain tissues (tumor vs non-tumor tissues), mice were sacrificed and brain tissue were excised at different time: D1, D7 and D11 or D12. In the radiosensitization study, tumors were irradiated at the total dose of 20 Gy (10 fractions of 2 Gy, once daily, 5 days/week over 2 weeks), as previously described [14].

evaluated for both liposomal doxorubicin was 24 mg/kg (*i.e.* total dose) with further dose escalation or de-escalation.

Determination of Intracranial Biodistribution of NPL-DXR and PL-DXR

Doxorubicin concentrations were measured in tissues of mice receiving intravenous injection of equitoxic doses of NPL-DXR and PL-DXR. In order to compare differential accumulation of DXR in brain tissues (tumor *vs* non-tumor tissues) during the treatment, DXR concentrations were assessed at different time after drug injection, as presented in Fig. 1. Hence, brain tissues, *i.e.* non-tumor brain hemisphere (NT) and tumor brain hemisphere (TT), were excised, washed in saline and immediately frozen at -20°C until processed. DXR concentration was determined by a reversed phase high performance liquid chromatography method after liquid-liquid extraction as described earlier [16]. In brief, tissues were homogenized in four parts of water. Homogenized tissue (0.5 ml) was then mixed with 500 ng daunorubicin as an internal standard, with 20 ml of AgNO_3 (33% in water), and with 8 ml of chloroform/isopropanol (1:1). After shaking for 20 min, the samples were centrifuged at $1,500\times g$ for 10 min, and the separated organic phase was evaporated under vacuum. Analyses were performed by reversed phase high-performance liquid chromatography on a C18 column

(250×4.6 mm I.D., YMC, Interchim, France), under isocratic elution conditions with a mobile phase of acetonitrile/0.01 mol/l KH_2PO_4 pH 2.6 (30:70) at a flow rate of 1 ml/min. DXR and daunorubicin were detected by a fluorescence detector (RF 10A XL Shimadzu, France) with excitation and emission wavelengths of 480 and 590 nm, respectively. The limit of detection of the assay was 2 ng/g of tissue. Areas under the curves (AUC) in tissues were determined based on median DXR concentrations using the Kinetica software (version 5.0 Adept Scientific).

Comparison of NPL-DXR and PL-DXR Effects on Radiotherapy Efficiency

Treatments started when presence of tumor was observed on MRI examination (Day-3), as previously described [14]. At D0 (corresponding to the first day of treatment), mice were randomly assigned into six groups. In the control group (CTRL), mice received injection with saline (0.9% NaCl). In the radiotherapy (RT) group, tumors were irradiated at the total dose of 20 Gy (10 fractions of 2 Gy, once daily, 5 days/week over 2 weeks), as previously described [17]. In the NPL-DXR and the PL-DXR groups, treatment schedules were defined according to the results of the distribution study. Hence, mice received injections of NPL-DXR at 24 mg/kg using 4 injections over two consecutive weeks. In the PL-DXR

groups, mice received injections at 15 mg/kg using 6 injections over two consecutive weeks. In the NPL-DXR + RT and PL-DXR + RT mice groups, liposomal doxorubicin was injected according to the earlier schedule during the entire ionizing radiation treatment.

When possible, MRI examination has been performed at the end of treatment (on day 14) allowing to assess the impact of treatments on tumor growth.

For the intracranial model, the mice were observed for body weight reduction. They were killed by cervical dislocation when they presented signs of neurological disorders or when their body weight reduction was more than 20% of their original weight, the time to this moment being referred to as “survival time”. The percentage of increase in the life span was calculated as $[(T - C)/C] \times 100$, where T and C are the median survival times of the treated and control animals.

Statistical Analysis

Kaplan–Meier curve analysis was performed using the Gehan–Breslow–Wilcoxon test. Statistical analysis was performed using GraphPad 5.0 software (GraphPad Prism 5.0 Software). Differences were considered significant at p values < 0.05 .

RESULTS

Our objective was to evaluate if liposomal doxorubicin (pegylated or not) could enhance the efficacy of a fractionated irradiation to treat high-grade glioma xenografts. To achieve the best radiosensitizing effect with liposomal DXR, the challenge was to identify the best therapeutic schedule allowing to (i) provide the best tumor exposure to DXR all along the radiation treatment course, (ii) avoid DXR accumulation in normal brain tissue. In the present study, NPL-DXR and PL-DXR have been evaluated and compared at their maximal tolerated dose (MTD). Two therapeutic schedules were assessed due to the difference in their circulation lifetime [18].

NPL-DXR and PL-DXR Equitoxicity

We first designed a dose ranging study to determine the maximal tolerated dose of each liposomal form in mice. We found that the MTD was 15 mg/kg for PL-DXR and 24 mg/kg for NPL-DXR, whatever the schedule (Table I). At these doses, neither weight loss more than 10% of initial body weight, nor toxic death occurred, avoiding the risk of failure for studies dealing with radiosensitizing potential.

NPL-DXR and PL-DXR Distribution in Brain Tissues

Based on these respective MTD, we attempted to determine the best profile of DXR exposure taking into account DXR accumulation in both non-tumor brain tissue (NT) and tumor brain tissue (TT). Evolution of DXR concentration in non-tumor and tumor hemispheres according to the therapeutic schedule (PL-DXR 4; PL-DXR 6; NPL-DXR 4; NPL-DXR 6) is reported in Fig. 2.

Median DXR concentrations were always higher in the tumor as compared to the normal cerebral tissue (Fig. 2a and b), even though the differences between both compartments were not constant all along the treatment sequence. This indicates a preferential liposomal DXR accumulation in tumor as compared to the normal brain tissue. At the end of the first week of treatment (Fig. 2c), differences between both tissues were maximal and the mean DXR concentration was about 5 times higher in tumor brain hemisphere than in the normal brain tissues. These differences were statistically significant, except for the PL-DXR form delivered in 4 injections (PL-DXR 4). For this last group, the calculated AUC after 2 weeks of treatments were 2,154 and 2,636 $\text{ng} \cdot \text{g}^{-1} \cdot \text{h}^{-1}$ in the non-tumor brain tissue and the tumor brain tissue ($\text{ratio AUC}_{\text{TT}}/\text{AUC}_{\text{NT}} = 0.82$), respectively (Table II), indicating that this schedule was not suitable for following experiments. When PL-DXR was fractionated into 6 injections (PL-DXR 6), the $\text{ratio AUC}_{\text{TT}}/\text{AUC}_{\text{NT}}$ has reached 2.56 which was more clinically acceptable: this more favorable ratio was due to differential accumulation of DXR in the normal brain tissue.

For the NPL-DXR-treated mice, the calculated AUC in tumor brain hemispheres were similar whatever the therapeutic schedule used (NPL-DXR 6: 7,173 $\text{ng} \cdot \text{g}^{-1} \cdot \text{h}^{-1}$ vs NPL-DXR 4: 6,779 $\text{ng} \cdot \text{g}^{-1} \cdot \text{h}^{-1}$). By contrast, the AUC in non-tumor brain hemispheres was increased in case of NPL-DXR 6 (NPL-DXR 6: 1,415 $\text{ng} \cdot \text{g}^{-1} \cdot \text{h}^{-1}$ vs NPL-DXR 4: 862 $\text{ng} \cdot \text{g}^{-1} \cdot \text{h}^{-1}$). Hence, the ratios have raised 7.86 and 5.07 for NPL-DXR 4 and NPL-DXR 6, respectively.

A statistically significant difference in DXR concentration in tumor hemisphere between NPL-DXR4 and PL-DXR6 groups was observed at the end of the first week of treatment ($p = 0.019$).

According to these results, we have chosen to study the effects of NPL-DXR 4 and PL-DXR 6 on radiotherapy efficiency, which corresponded to the best potential accumulation of DXR within the tumor hemisphere during the treatment course.

Comparison of NPL-DXR and PL-DXR Effects on Radiotherapy Efficiency

The endpoint of this study was the overall survival analyzed by the Kaplan–Meier method (Table III; Fig. 3). In the untreated

Table 1 Evaluation of the Maximum Tolerated Dose (MTD) to Define the Equitoxicity of PL-DXR and NPL-DXR

Treatment groups		Toxic deaths		Initial mice weight (g)		Weight loss (%) during the treatment		Mice general status	Conclusion
Drug	Total doses and schedules	Number of deaths/ Number of mice	Day of death	Mean	Range	Mean	Range		
PL-DXR	24 mg/kg	1/3	D38	N/A	N/A	N/A	N/A	altered	Toxicity
	3 injections/week × 2 weeks								
	24 mg/kg	1/3	D34	N/A	N/A	N/A	N/A	altered	Toxicity
	2 injections/week × 2 weeks								
	18 mg/kg	1/11	D32	28.9	27.8–30.0	6.5%	1–10.1	good	Toxicity
	3 injections/week × 2 weeks								
	18 mg/kg	1/11	D20	29.3	28.0–30.3	8.2%	0–12.5	good	Toxicity
	2 injections/week × 2 weeks								
	15 mg/kg	0/7		26.9	25.6–27.5	4.7%	0–6.0	good	MTD
	3 injections/week × 2 weeks								
	15 mg/kg	0/7		28.4	26.7–30.5	3.5%	0–6.7	good	MTD
	2 injections/week × 2 weeks								
	12 mg/kg	0/7		26.9	26.0–28.6	1.4%	0–4.0	good	well-tolerated
	3 injections/week × 2 weeks								
	12 mg/kg	0/7		27.4	25.4–30.4	2.0%	0–5.6	good	well-tolerated
	2 injections/week × 2 weeks								
NPL-DXR	36 mg/kg	2/4	D17 and D24	28.9	25.4–33.3	21.0%	9.5–28.7	altered	Toxicity
	3 injections/week × 2 weeks								
	36 mg/kg	3/4	D13, D20 and D22	30.0	27.7–32.7	20.7%	11.3–38	altered	Toxicity
	2 injections/week × 2 weeks								
	30 mg/kg	2/10	D7 and D18	29.2	28.9–30.9	9.6%	0–22.5	good	Toxicity
	3 injections/week × 2 weeks								
	30 mg/kg	3/10	D7, D15 and D18	29.4	26.5–32.3	19.3%	7.6–31.3	good	Toxicity
	2 injections/week × 2 weeks								
	24 mg/kg	0/7		26.0	24.8–26.9	1.7%	0–5.0	good	MTD
	3 injections/week × 2 weeks								
	24 mg/kg	0/7		26.3	24.7–28.8	6.0%	0–9.4	good	MTD
	2 injections/week × 2 weeks								

CTRL group, the median survival was 27 days. Administered alone, both NPL-DXR and PL-DXR improved mice survival to 36 days and 40 days, respectively. This corresponds to an increase in life span of 25 and 32%, respectively, but the difference with the CTRL group reaches the level of statistical significance only for PL-DXR ($p=0.032$). Overall survival was slightly decreased (18%) when mice received RT alone (22 days) as compared with CTRL group without clear explanation.

Median survival was 47 days for the NPL-DXR 4 + RT group and 48 days for the PL-DXR 6 + RT group. These results highlight a synergistic interaction between liposomal DXR and ionising radiation, even though the statistical significance was only raised for NPL-DXR ($p=0.042$ as compared to RT alone). The improvement in overall survival probably resulted from a slowing of the tumor growth, as shown in Fig 3c.

DISCUSSION

Due to their dose-limiting cardiotoxicity, vectorization of anthracyclins remains a major challenge in oncology. In this

context, many articles are published each year to report new anthracyclin-loaded nano-carriers or new vectorization strategies [19–21]. While the free doxorubicin freely distributes in the body, drug-loaded nano-carriers accumulate in tissues with functionally porous vasculature such as liver and spleen and with leaky vasculature such as tumors. In preclinical studies, an increased concentration of DXR has been obtained in intracerebral tumor models [7, 8, 14], and was linked to an improved therapeutic efficacy for PL-DXR in intracranial glial tumor models [7, 22]. In this context, recent works have demonstrated the interest of combining liposomal doxorubicin with ultrasound-induced disruption of blood-tumor and blood-brain barrier to improve outcome in glioma-bearing rats [23, 24]. However, these promising results have not been translated into clinical benefit: PL-DXR only produced a modest increase in survival when administered alone in patients with recurrent high grade gliomas [9, 10], despite enhanced tumor exposure to doxorubicin [25]. Based on these conclusions and the well-established role of concomitant radio-chemotherapy in the treatment of glioblastoma, liposomal doxorubicin was assessed in a concomitant association with fractionated irradiation in our model of malignant

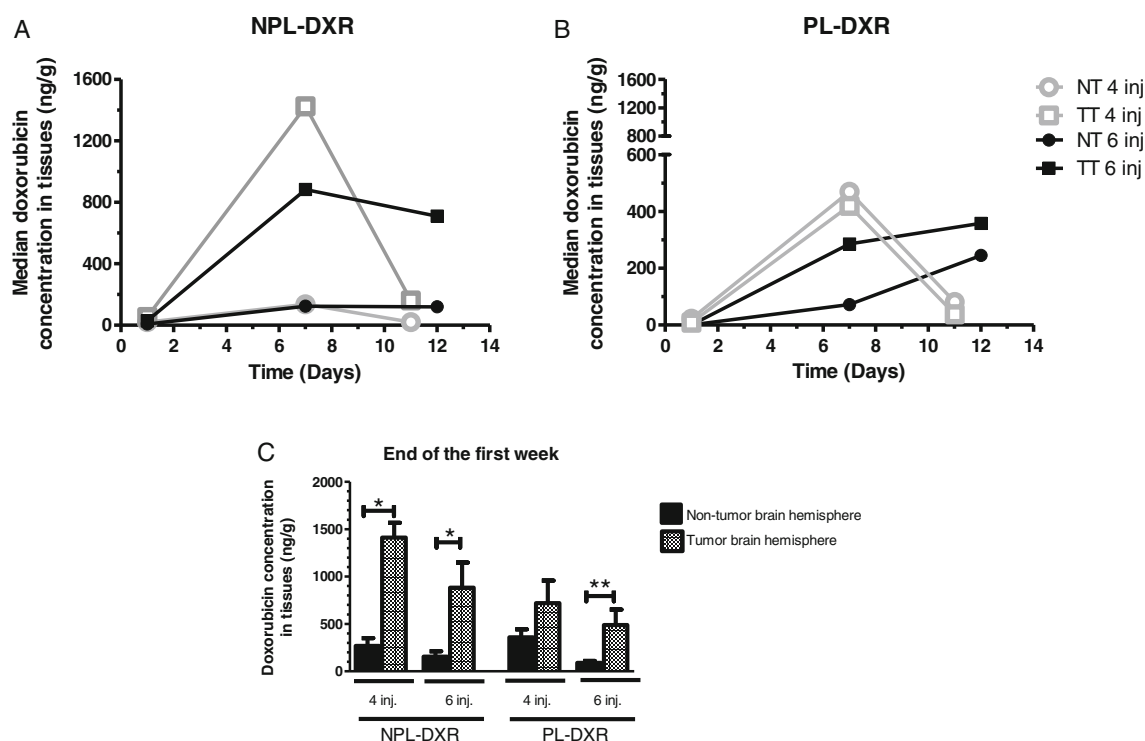


Fig. 2 Determination of DXR concentration in brain tissues. Doxorubicin concentrations were measured in both tumor brain hemisphere (TT) and non-tumor hemisphere (NT) of mice after intravenous injection of liposomal doxorubicin. Median DXR concentrations were determined on days D1, D7 and D11 or D12 after **(a)** NPL-DXR or **(b)** PL-DXR administration. NPL-DXR and PL-DXR were injected at the maximal tolerated dose, i.e. 24 and 15 mg/kg, respectively, fractionated in 4 or 6 injections over 2 weeks. DXR concentrations were determined by a reversed phase high performance liquid chromatography method after liquid–liquid extraction as described earlier [14]. **(c)** Comparison of mean DXR concentrations in tumor and non-tumor brain tissues at the end of the first week of treatment (D7).

glioma xenografts. Moreover, the ability of liposomal forms to act as a depot preparation for sustained intratumoral doxorubicin release was expected beneficial in case of daily fractionation of the radiation therapy: each fraction of irradiation would be delivered while the drug is present in the tumor.

While doxorubicin has been demonstrated to enhance the therapeutic effect of RT on different models of cancers [11–13, 26], we have previously showed that the vectorization is absolutely necessary to allow the combination of doxorubicin and radiation therapy in high grade gliomas *in vivo* [14]: indeed, concomitant association of free DXR with fractionated irradiation has led into toxic death in 100% of mice. By contrast, when administered in combination with fractionated irradiation, NPL-DXR was shown to significantly radiosensitize two models of malignant glioma (TCG4 and

U87) when subcutaneously xenografted: for U87 tumor bearing-mice, an increase of about 37% in life span has been observed for U87 tumor bearing-mice, as compared to those receiving RT alone. However, these results could not be reproduced on the U87 intracranial model, likely due to the lack of therapeutic schedule optimization.

Hence, to provide radiosensitization at best, the challenge is to select the more suitable anthracyclin-loaded carrier with the best therapeutic schedule. Unfortunately, few studies were designed to compare different drug-loaded carriers concerning their distribution abilities, their tumor accumulation profile or their antitumor efficacy alone or in combination [18, 27, 28].

The present study was designed to evaluate the efficiency of conventional or pegylated liposomal doxorubicin combined

Table II Brain Tissues Exposure to Doxorubicin Expressed Through Areas Under the Curve (AUC)

	NPL-DXR 4	NPL-DXR 6	PL-DXR 4	PL-DXR 6
Non-tumor brain hemisphere (NT)	862	1,415	2,636	1,031
Tumor brain hemisphere (TT)	6,779	7,173	2,154	2,637
Ratio AUC _{TT} /AUC _{NT}	7.86	5.07	0.82	2.56

NPL-DXR at the maximal tolerated dose (total dose = 24 mg/kg) fractionated into 4 or 6 injections; PL-DXR at the maximal tolerated dose (total dose = 15 mg/kg) fractionated into 4 or 6 injections. The AUC were determined based on median DXR concentrations using the Kinetica software

Table III Median Overall Survival According to Treatment Groups

	CTRL	NPL-DXR 4	PL-DXR 6	RT	RT + NPL-DXR 4	RT + PL-DXR 6
Median survival (days)	27	36	40	22	47	48
Long survivors (> 180 days)	0/7	0/7	0/7	0/7	2/7	2/7

NPL-DXR at the maximal tolerated dose (total dose = 24 mg/kg) fractionated into 4 injections; PL-DXR at the maximal tolerated dose (total dose = 15 mg/kg) fractionated into 6 injections; Radiotherapy was delivered at the dose of 2 Gy/fraction/day over 5 days. All the treatments were delivered on two consecutive weeks

with radiotherapy in orthotopic high-grade glioma xenografts. The pegylated liposomal doxorubicin (PL-DXR, Caelyx®) approved in the US is coated with surface-bound methoxypolyethylene glycol while the non pegylated form (NPL-DXR, Myocet®), approved in Europe, is encapsulated in liposomal membrane of phosphatidylcholine and cholesterol. Their described sizes were ~100 and ~160 nm, respectively [29, 30]. The major difference between pegylated- and conventional liposomes is the reduced uptake by the reticulo-endothelial system of pegylated liposomes, involving distinct blood circulation lifetime [31]. However, little is known about their respective distribution in normal brain and brain tumors as no comparison of these two agents have already been made on a same intracerebral tumor model. Hence, to compare their radiosensitizing effect, it was first necessary to determine

the optimal schedule and dosing of drug delivery for each liposomal form. Given that these two formulations have distinct pharmacokinetic and toxicity profiles [18, 32], the distribution in normal and tumor brain tissues needs to be assessed at equitoxic total dose using different schedules, as previously reported [27].

Our MTD study using two schedules of both PL-DXR and NPL-DXR showed that to obtain the same profile of toxicity, the maximum tolerated dose of NPL-DXR is about 37% higher than those of the pegylated form. This preclinical observation is in agreement with reported results of clinical trials wherein the well tolerated dose is about 45 and 60 mg/m² respectively for Caelyx® and Myocet®. It should be noticed that the schedule had no influence on the MTD, whatever the liposomal formulation.

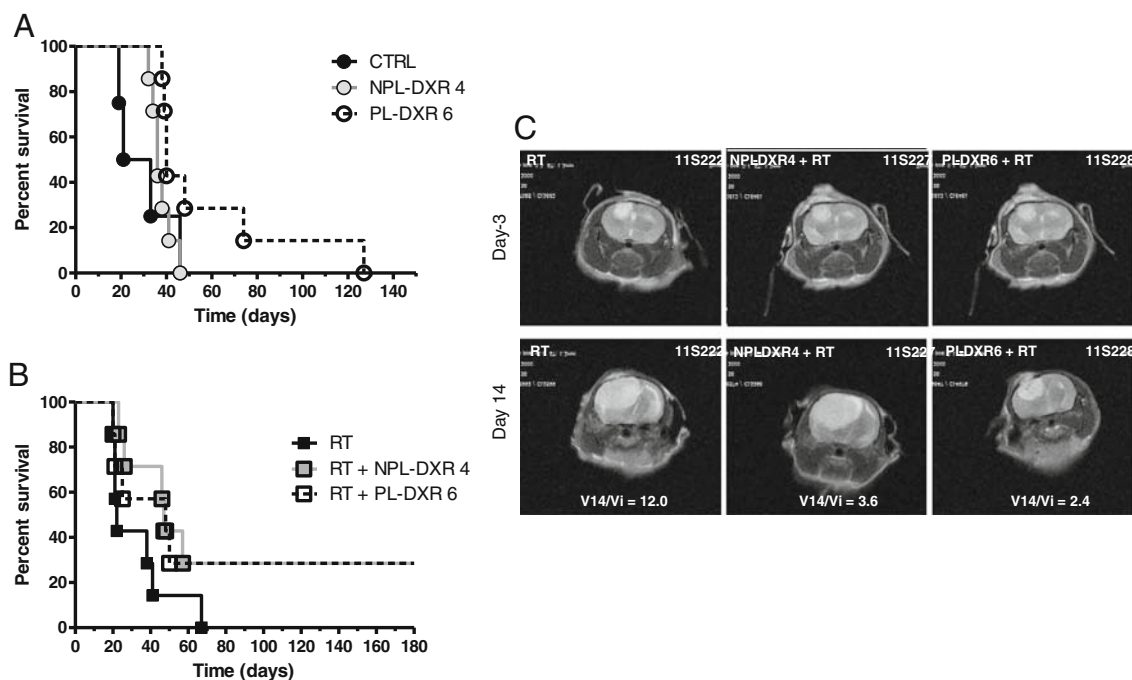


Fig. 3 Response of U87 intracranial xenografts to antitumoral treatments. Intracranial U87 tumor-bearing mice were randomly assigned into four groups when tumors were observed on MRI examination: control (CTRL) ($n = 6$), NPL-DXR ($n = 7$), PL-DXR ($n = 7$), radiation therapy (RT) ($n = 7$), NPL-DXR + RT ($n = 7$), and PL-DXR + RT ($n = 7$). Tumors were irradiated at the total dose of 20 Gy (10 fractions of 2 Gy, once daily, 5 days/week over 2 weeks). NPL-DXR was injected at the maximal tolerated dose of 24 mg/kg fractionated in 4 injections over 2 weeks. PL-DXR was injected at the maximal tolerated dose of 15 mg/kg fractionated in 6 injections over 2 weeks. The effects of treatments on overall survival are represented as Kaplan–Meier plots. Kaplan–Meier curves were plotted for mice treated (a) by injection of liposomal DXR as compared to saline (CTRL); (b) by irradiation in combination with liposomal DXR, as compared to RT alone. (c) Representative images obtained by MRI examination for intracerebral U87 xenografts before treatment onset (Day-3) and at the end of treatment (Day 14). The ratio between final tumor volume (V_{14}) and initial tumor volume (V_i) were calculated to assess the tumor growth.

As external beam irradiation is a non-selective treatment for brain tumor, it is necessary to determine the best compromise between high tumor drug accumulation and low normal brain exposure. Doxorubicin concentrations were always higher in the tumor brain hemisphere than in the normal tissue, except for the PL-DXR4 group (herein, concentrations were unexpectedly similar and need further histological investigations). These results confirm the preferential DXR accumulation in tumor tissue, in accordance with the previously published results [7, 33]. The leaky vasculature that characterizes high-grade gliomas allows the liposomes deposit in tumor tissue, in contrast to the blood brain barrier perfectly sealed in normal brain. These results were confirmed in clinical studies. Koukourakis *et al.* have used planar and SPECT scintigraphy to investigate the relative accumulation of the radiolabelled PL-DXR in tumor and normal brain areas in 5 patients with glioblastoma [25]. The PL-DXR accumulation was 7–13 times higher in the glioblastoma as compared to the normal brain tissue.

The better differential over the treatment course ($ratio AUC_{TT}/AUC_{NT}=7.86$) and the highest concentrations were obtained with NPL-DXR 4. However, the difference in DXR accumulation between both tissues was maximal at the end of the first week, and decreased at the end of the second week, that may evoke the activation of resistance mechanisms involving efflux pump such as P-glycoprotein [34].

Consistently with previous published works [7, 22, 23], the increased concentrations of DXR in the present study were linked to an improved therapeutic efficacy in intracranial glial tumor model. Actually, while administered alone, both NPL-DXR 4 and PL-DXR 6 slightly improved mice survival, even though the difference was more marked and significant for PL-DXR 6. In their phase II clinical trial, Fabel *et al.* have reported long-term stabilization in 54% of patients with recurrent malignant glioma after treatment with Caelyx® [9].

As expected, a supra-additive effect was observed when RT was combined with NPL-DXR 4 and PL-DXR 6: median overall survival was 2-fold increased for mice treated with combined therapies, as compared to RT alone. These results confirm the radiosensitizing potential of NPL-DXR that was observed on subcutaneous U87 xenografts in our first study. The present work highlights the importance of using appropriate therapeutic schedule and dosing to achieve the best radiosensitizing effect in intracranial model. In the present study, the dose of NPL-DXR is twice higher (total cumulative dose: 24 vs 12 mg/kg) than used in our first study, that may lead to higher DXR concentrations within the tumor. To our knowledge, no other study has reported the use of such an association (NPL-DXR or PL-DXR + RT) in a malignant glioma orthotopic xenografts model. An increase in RT effect by PL-DXR on human osteosarcoma, head and neck and prostate cancer xenograft models have been described [11–14].

In the clinical study of Koukourakis *et al.*, four complete and two partial responses were obtained out of 10 patients harboring brain metastasis (breast, non-small cell lung carcinomas) treated with PL-DXR combined with radiotherapy, but none of five patients treated for a glioblastoma responded while the drug accumulation was significantly higher in glioblastomas [25]. However, the role of DXR encapsulation for the treatment of brain tumors is running using, in particular, nanoparticles made up various biodegradable polymers [2, 35].

In conclusion, the present study has shown that both the pegylated and non pegylated liposomal forms of DXR allow higher DXR accumulation in brain tumors as compared to the normal brain tissue providing a strong background for using their concomitant combination with radiotherapy. We demonstrated a radiosensitizing effect without toxicity of this combination on a human malignant glioma orthotopic xenograft. However, this radiosensitization depends greatly on the schedule and the dosing of liposomal doxorubicin. This study shows that the use of nanocarriers, allowing targeting of intracerebral tumor, renders relevant the combination of anthracyclin with radiation therapy to treat brain tumors, opening a new field of therapeutic applications. However, our results point out that, for each new delivery system, the administration schedules need to be rigorously optimized. These interesting results should encourage the design of phase I trials of radiochemotherapy using liposomal forms of DXR for the treatment of malignant brain tumors.

ACKNOWLEDGMENTS AND DISCLOSURES

We are very grateful to the French “Ligue Contre le Cancer, Comités Lorrains” for financial supports. We thank S. Leclerc and J.M. Escanyé (Service Commun de RMN, Institut Jean Barriol, Université de Lorraine) for technical assistance.

REFERENCES

1. Stupp R, Hegi ME, Mason WP, van den Bent MJ, Taphoorn MJ, Janzer RC, *et al.* Effects of radiotherapy with concomitant and adjuvant temozolomide versus radiotherapy alone on survival in glioblastoma in a randomised phase III study: 5-year analysis of the EORTC-NCIC trial. *Lancet Oncol.* 2009;10(5):459–66.
2. Kreuter J. Drug delivery to the central nervous system by polymeric nanoparticles: what do we know? *Rev. Adv. Drug. Deliv.* 2013. doi: 10.1016/j.addr.2013.08.008.
3. Wolff JE, Trilling T, Molenkamp G, Egeler RM, Jurgens H. Chemosensitivity of glioma cells in vitro: a meta-analysis. *J Cancer Res Clin Oncol.* 1999;125(8–9):481–6.
4. Veringa SJ, Biesmans D, van Vuurden DG, Jansen MH, Wedekind LE, Horsman I, *et al.* In vitro drug response and efflux transporters

- associated with drug resistance in pediatric high grade glioma and diffuse intrinsic pontine glioma. *PLoS One*. 2013;8(4):e61512.
5. Lesniak M, Upadhyay U, Goodwin R, Tyler B, Brem H. Local delivery of doxorubicin for the treatment of malignant brain tumors in rats. *Anticancer Res*. 2005;25(6B):3825–31.
 6. Voulgaris S, Partheni M, Karamouzis M, Dimopoulos P, Papadakis N, Kalofonos HP. Intratumoral doxorubicin in patients with malignant brain gliomas. *Am J Clin Oncol*. 2002;25(1):60–4.
 7. Siegal T, Horowitz A, Gabizon A. Doxorubicin encapsulated in sterically stabilized liposomes for the treatment of a brain tumor model: biodistribution and therapeutic efficacy. *J Neurosurg*. 1995;83(6):1029–37.
 8. Anders CK, Adamo B, Karginova O, Deal AM, Rawal S, Darr D, et al. Pharmacokinetics and efficacy of PEGylated liposomal doxorubicin in an intracranial model of breast cancer. *PLoS One*. 2013;8(5).
 9. Fabel K, Dietrich J, Hau P, Wismeth C, Winner B, Przywara S, et al. Long-term stabilization in patients with malignant glioma after treatment with liposomal doxorubicin. *Cancer*. 2001;92(7):1936–42.
 10. Hau P, Fabel K, Baumgart U, Rümmele P, Grauer O, Bock A, et al. Pegylated liposomal doxorubicin efficacy in patients with recurrent high-grade glioma. *Cancer*. 2004;100(6):1199–207.
 11. Harrington KJ, Rowlinson-Busza G, Syrigos KN, Vile RG, Uster PS, Peters AM, et al. Pegylated liposome-encapsulated doxorubicin and cisplatin enhance the effect of radiotherapy in a tumor xenograft model. *Clin Cancer Res*. 2000;6(12):4939–49.
 12. Davies CL, Lundstrom LM, Frengen J, Eikenes L, Bruland SOS, Kaalhus O, et al. Radiation improves the distribution and uptake of liposomal doxorubicin (Caelyx) in human osteosarcoma xenografts. *Cancer Res*. 2004;64(2):547–53.
 13. Hagtvet E, Røe K, Olsen DR. Liposomal doxorubicin improves radiotherapy response in hypoxic prostate cancer xenografts. *Radiat Oncol*. 2011;6:135–45.
 14. Labussière M, Aarnink A, Pinel S, Taillandier L, Escanyé JM, Barberi-Heyob M, et al. Interest of liposomal doxorubicin as a radiosensitizer in malignant glioma xenografts. *Anticancer Drugs*. 2008;19(10):991–8.
 15. Pinel S, Barberi-Heyob M, Cohen-Jonathan E, Merlin JL, Delmas C, Plenat F, et al. Erythropoietin-induced reduction of hypoxia before and during fractionated irradiation contributes to improvement of radioresponse in human glioma xenografts. *Int J Radiat Oncol Biol Phys*. 2004;59(1):250–9.
 16. Meco D, Colombo T, Ubezio P, Zucchetti M, Zaffaroni M, Riccardi A, et al. Effective combination of ET-743 and doxorubicin in sarcoma: preclinical studies. *Cancer Chemother Pharmacol*. 2003;52(2):131–8.
 17. Pinel S, Mriouah J, Vandamme M, Chateau A, Plenat F, Guérin E, et al. Synergistic antitumor effect between gefitinib and fractionated irradiation in anaplastic oligodendrogliomas cannot be predicted by the EGFR signaling activity. *PLoS One*. 2013;8:e68333.
 18. Hong RL, Huang CJ, Tseng YL, Pang VF, Chen ST, Liu JJ, et al. Direct comparison of liposomal doxorubicin with or without polyethylene glycol coating in C-26 tumor-bearing mice: is surface coating with polyethylene glycol beneficial? *Clin Cancer Res*. 1999;5(11):3645–52.
 19. Pramanik D, Campbell NR, Das S, Gupta S, Chenna V, Bisht S, et al. A composite polymer nanoparticle overcomes multidrug resistance and ameliorates doxorubicin-associated cardiomyopathy. *Oncotarget*. 2012;3(6):640–50.
 20. Golla K, Cherukuvada B, Ahmed F, Kondapi AK. Efficacy, safety and anticancer activity of protein nanoparticle-based delivery of doxorubicin through intravenous administration in rats. *PLoS One*. 2012;7(12):e51960.
 21. Tacar O, Sriamornsak P, Dass CR. Doxorubicin: an update on anticancer molecular action, toxicity and novel drug delivery systems. *J Pharm Pharmacol*. 2013;65(2):157–70.
 22. Sharma US, Sharma A, Chau RI, Straubinger RM. Liposome-mediated therapy of intracranial brain tumors in a rat model. *Pharm Res*. 1997;14(8):992–8.
 23. Aryal M, Vykhodtseva N, Zhang YZ, Park J, McDannold N. Multiple treatments with liposomal doxorubicin and ultrasound-induced disruption of blood-tumor and blood-brain barriers improve outcomes in a rat glioma model. *J Control Release*. 2013;169(1–2):103–11.
 24. M. Aryal, C. D. Arvanitis, P. M. Alexander, N. McDannold. Ultrasound-mediated blood-brain barrier disruption for targeted drug delivery in the central nervous system. *Adv. Drug Deliv. Rev.* (2014).
 25. Koukourakis MI, Koukouraki S, Fezoulidis I, Kelekis N, Kyrias G, Archimandritis S, et al. High intratumoural accumulation of stealth liposomal doxorubicin (Caelyx) in glioblastomas and in metastatic brain tumours. *Brit J Cancer*. 2000;83(10):1281–6.
 26. Chastagner P, Labussière M, Aarnink A, Pinel S, Fouyssac F, Bernier V. Comparison of doxorubicin and a liposomal form, doxorubicin chlorhydrate, as radiosensitizer in high grade glioma and rhabdomyosarcoma xenografts. *Int J Radiat Oncol Biol Phys*. 2006;66: S579.
 27. Parr MJ, Masin D, Cullis PR, Bally MB. Accumulation of liposomal lipid and encapsulated doxorubicin in murine Lewis lung carcinoma: the lack of beneficial effects by coating liposomes with poly(ethylene glycol). *J Pharmacol Exp Ther*. 1997;280(3):1319–27.
 28. Hendriks BS, Reynolds JG, Klinz SG, Geretti E, Lee H, Leonard SC, et al. Multiscale kinetic modeling of liposomal doxorubicin delivery quantifies the role of tumor and drug-specific parameters in local delivery to tumors. *Pharmacometrics Syst Pharmacol*. 2012;1:e15.
 29. Charrois GJ, Allen TM. Multiple injections of pegylated liposomal doxorubicin: pharmacokinetics and therapeutic activity. *J Pharmacol Exp Ther*. 2003;306(3):1058–67.
 30. Charrois GJ, Allen TM. Rate of biodistribution of STEALTH liposomes to tumor and skin: influence of liposome diameter and implications for toxicity and therapeutic activity. *Biochim Biophys Acta*. 2003;1609(1):102–8.
 31. Allen TM, Cullis PR. Liposomal drug delivery systems: from concept to clinical applications. *Adv Drug Deliv Rev*. 2013;65(1):36–48.
 32. Duggan ST, Keating GM. Pegylated liposomal doxorubicin: a review of its use in metastatic breast cancer, ovarian cancer, multiple myeloma and AIDS-related Kaposi's sarcoma. *Drugs*. 2011;71(18):2531–58.
 33. Arnold RD, Mager DE, Slack JE, Straubinger RM. Effect of repetitive administration of Doxorubicin-containing liposomes on plasma pharmacokinetics and drug biodistribution in a rat brain tumor model. *Clin Cancer Res*. 2005;11(24 Pt 1):8856–65.
 34. Tsuji A. P-glycoprotein-mediated efflux transport of anticancer drugs at the blood-brain barrier. *Ther Drug Monit*. 1998;20(5):588–90.
 35. Wohlfart S, Gelperina S, Kreuter J. Transport of drugs across the blood-brain barrier by nanoparticles. *J Control Release*. 2012;161(2):264–73.